Mechanical and Chemical Characterisation of Bioresorbable Polymeric Stent over Two-year *in vitro* Degradation

R Naseem[1], LG Zhao[1*], VV Silberschmidt[1], Y Liu[1], OW Scaife[2], H Willcock[2], SK Eswaran[3], S Hossainy[3]

[1]Wolfson School of Mechanical, Electrical and Manufacturing Engineering, Loughborough University, Loughborough, LE11 3TU, UK

[2]Department of Materials, Loughborough University, Loughborough, LE11 3TU, UK

[3]Abbott Vascular, 3200 Lakeside Drive, Santa Clara, CA 95054, USA

[*]Corresponding author, Email: L.Zhao@Lboro.ac.uk, Tel: 0044-1509-227799

Abstract

Polymeric stent is a temporary cardiovascular scaffold, made of biodegradable poly (l-lactic) acid, to treat coronary artery stenosis, with expected resorption by the human body over two to three years. In this paper, the mechanical properties of a polymeric stent over two-year *in vitro* degradation were studied and characterised using atomic force microscopy and nanoindentation techniques, complemented with analyses of weight loss, gel permeation chromatography and differential scanning calorimetry. Atomic force microscopy assessed stent degradation at the surface, whilst nanoindentation was able to investigate the property at a greater depth into the [illegible] the atomic force microscopy due to bulk degradation nature of the polymer. Chemical analyses demonstrated a reduction of molecular weight and an increase of crystallinity, indicating degradation of the stents. Berkovich nanoindentation showed a trend of reduction in modulus over *in vitro* degradation, which was, however, not continuous due to the variations of measurements associated with the pyramidal indenter tip and the semi-crystalline structure of the polymer.

Keywords: Polymeric stent; Material properties; Berkovich nanoindentation; Atomic force microscopy; *in vitro* degradation

1. Introduction

Biodegradable polymers are used for a range of medical devices, including sutures and implantable scaffolds [1]. Polylactides is a common polymer group used extensively in these applications. The chiral nature of polylactides (polyester) results in multiple structural forms of the molecule, with poly (L-lactic acid) (PLLA) shown to be the most promising for stent applications [2-5]. PLLA has an intrinsic degradation property, and the material can be broken down, excreted or resorbed by the metabolic pathways within the body without surgical intervention [1]. Here, degradation is defined as the chain scission process, during which polymer chains are cleaved to form oligomers and monomers [6]. Due to hydrolysable bonds within the polymer, there are two possible means of chain cessation, i.e., chemical degradation via hydrolysis or enzyme catalysed hydrolysis, with the former being more prominent for the degradation of bioresorbable stents [7, 8].

Degradation of PLLA has been studied in various forms, encompassing fibers, thin films and bulk specimens. Yuan *et al.* [9] assessed *in vitro* degradation of PLLA fibers incubated in phosphate buffer solution (PBS) at 7.4 pH level and 37°C for up to 45 weeks. Three kinds of fibers with varying diameters and molecular weights were investigated. It was shown that their average molecular weight decreased progressively with degradation, with a drop of 39.3% - 57.9% for the three fiber sets. Despite this molecular weight regression, corresponding decrease in respective masses was not observed for any of the fiber sets. An increase in crystallinity was demonstrated with differential scanning calorimetry (DSC), which corresponded to an increase in molecular order of polymeric chains in semi-crystalline structures. Tensile properties were also assessed for these fibers; however, there were no significant changes after 35 weeks of *in vitro* degradation for

thicker strands. Thinner fiber strands showed a decrease in ultimate strength with respect to initial values. Nuutinen *et al.* [10] assessed the mechanical properties and *in vitro* degradation of PLLA bioresorbable knitted stents, constructed using single self-reinforced fibers. The *in vitro* degradation of the PLLA fibers showed a decline in ultimate tensile strength, with a decrease from ~300 MPa to 0 MPa over the course of 35 weeks. Similar to the work of Yuan *et al.*[9], the molecular weight of the PLLA fibers diminished over a 50-week period but 90% of its mass was retained over the same time period. Even after 110 weeks of *in vitro* degradation, the PLLA scaffold maintained 59% of its mass. Zilberman *et al.* [11] investigated the mechanical properties and *in vitro* degradation of PLLA bioresorbable fibers, which showed excellent biocompatibility and high tensile mechanical properties (a tensile strength of 967 MPa and a modulus of 5 GPa). During the 6-week *in vitro* degradation, PLLA showed no weight loss while tensile testing of the fibers exhibited a 30.1% and 8.9% drop in tensile strength and modulus, respectively.

In addition, Jowsa *et al.* [12] discussed how changes within the core of a biodegradable polymer can be attributed to its amorphous fraction which is capable of absorbing more water, therefore affecting degradation and material properties. In their study, PLLA was produced by injection moulding. The reduction in strength was less than 10% after a five-month incubation period, proving advantageous for supporting vessel wall regeneration. Luo *et al.* [13] tested the behaviour of polymeric stents, made of ultra-high-molecular-weight PLLA, both *in vitro* and *in vivo*. For *in vitro* study, the stents were integrated into a customary system, consisting of a plasma pump and a mock artery loop, to simulate the *in vivo* environment. Flow pressure applied was equal to that of the human circulatory system, with the temperature and pH level of the system regularly monitored. For assessment of *in vivo* degradation, stents were implanted into pig arteries of similar dimensions to the mock arteries. The degradation of stents was assessed under both *in vitro* and *in vivo* conditions, showing good agreement with each other in terms of the change of stent outer

diameter and the reduction of molecular weight at 1, 3 and 6 months; however, there was no information on the rate or characteristics of stent degradation.

PLLA used in the biomedical field is usually tailored for a specific application, and therefore, results presented in literature are specific for the materials studied and cannot be generalised. This is due to different processing, manufacturing and sterilization conditions which affect material properties as a result of the variation in crystallinity [14]. Ghosh *et al.* [15] demonstrated that melt processing of polymers can degrade the material and therefore, change its properties. Also, existing work is largely limited to the polymer fibers or bulk samples, and there is a lack of study regarding the degradation of polymeric stents in their manufactured states, especially the change of material properties over degradation. In this paper, properties of PLLA biodegradable stent were assessed over degradation under *in vitro* conditions. Efforts were made to assess the local properties of polymeric stent, at different length scales (200 nm to 4 μm), in manufactured states. The work covers assessment of its surface properties via profilometry and indentation studies at different depths. Both atomic force microscopy (AFM; 200 nm) and nanoindentation (up to 4 μm) were carried out to assess the material properties over two-year *in vitro* degradation. The work was complemented with chemical analyses to quantify the molecular-weight loss and crystallinity variation over the degradation process.

2. Experiments

2.1 Material and samples

The samples for the *in vitro* degradation study were poly-lactic acid (PLLA) stent (Fig. 1a) supplied by Abbott Vascular (California, USA). The wall thickness for the stent is ~150 μm and the strut width is ~200 μm, confirmed also with optical imaging (SmartScope Flash 200). Stent sections containing 3-4 rings were produced using a sharp blade in a sterile environment and incubated in glass vials containing phosphate buffer solution (PBS) at 37°C (Fig. 1b). PBS was changed monthly

to maintain a neutral pH level (~7.4) throughout incubation. This was determined after carrying out a pre-testing study (i.e., a set of simple tests to determine if the pH level would change with incubation time), which found insignificant pH changes over one-month period. Indicator sticks (Fisher brand) were also used to monitor pH level over the duration of the study to guarantee neutrality. Assessment of stent rings was carried out at monthly intervals.

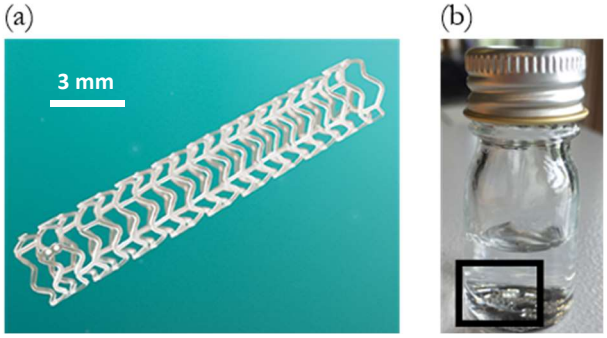

Figure 1, (a) Polymer stent and (b) ring section in a vial filled with PBS.

2.2 Surface Profilometry

Roughness measurements were carried out using a ContourGT-X 3D optical profilometer (Bruker, U.S.A) to assess the surface topography. These non-contact surface measurements and characterisation of surface features were carried out for samples in virgin and degraded states. In particular, the arithmetic average of absolute values of height deviations from a mean line, i.e., R_a, was evaluated over a desired length. In this study, five measurements were taken randomly across the outer surfaces of the stent. Data was analysed using the Vision64 Map Software and MountainsMap Universal (Digital Surf).

2.3 Atomic Force Microscopy (AFM)

Surface indentations were carried out using an AFM Explorer (Veeco), with indents made on three locations across the stent, i.e., a tri-junction, a straight strut and a U-bend (Fig. 2). 20 indents were

made at each location randomly using a silicon tip with a radius of 10 nm. A 10 nN load was set, and the corresponding displacement was recorded during loading and unloading. A 200 nm offset was applied to counteract the effect of any possible contamination, which might be present on the sample surface. Indents were made on surfaces normal to both the radial and longitudinal axes of the stent to assess variability in these two directions. Using a method proposed by Tang *et al.* [16], the elastic modulus of the material was calculated on the basis of Sneddon's elastic contact solution:

$$E_r = \frac{\alpha}{K/A - 1} \tag{1}$$

$$\frac{1}{E_r} = \frac{(1-\nu^2)}{E} + \frac{(1-\nu_i^2)}{E_i} \quad , \tag{2}$$

where E_r is the reduced modulus of the material related to the contact between the tip and the sample, E and ν are elastic modulus and Poisson's ratio of the material, E_i and ν_i are the elastic modulus and the Poisson's ratio of the indenter tip (137 GPa and 0.17, respectively [16]). The two parameters α and A define the cantilever-tip property and cantilever sensitivity, respectively. They were obtained through carrying out AFM tests on two reference materials with the known moduli. Here, poly (methyl methacrylate) (PMMA) and polystyrene (PS) were considered with a modulus of 2.76 GPa and 3.55 GPa, respectively, which were obtained using dynamic mechanical analysis (DMA). The parameter K was defined as the gradient of the unloading curve obtained with AFM. Once these values are known, they can be used to quantify the unknown elastic modulus of a material using equation (2). The assumption is made that no plastic deformation of the tip occurs during this calibration procedure [16]. Stent rings were mounted onto metallic rod, which exactly fit the inner area of the stent to ensure support of the stent during indentation.

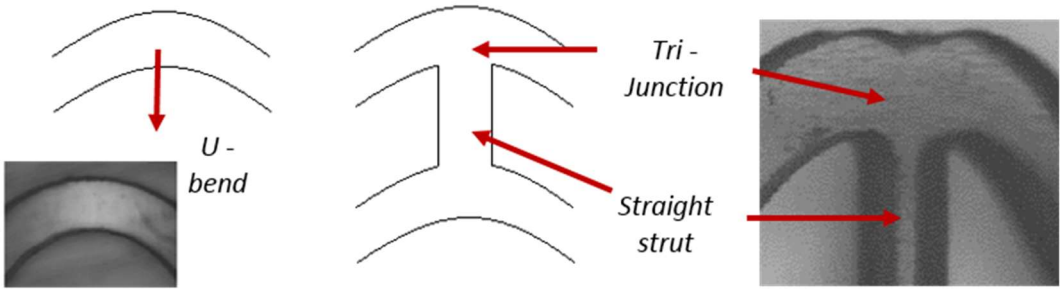

Figure 2, Images and schematic of the areas of interest across the stent.

2.4 Nanoindentation

Nanoindentation was performed using a Platform 3 indenter (Micromaterials, Wrexham). This was carried out on a nanoscale using a Berkovich tip. A loading rate of 0.5 mN/s and an unloading rate of 5 mN/s were chosen, with a 40-second dwell time at the level of maximum loading. To allow for correction of indentation data with regard to thermal drift, a hold phase of 60 s was implemented at 80% of unloading. The elastic modulus of the materials was determined using the Oliver-Pharr theory, based on the slope of the unloading curve (top portion; 20%) [17]. Using equation (2), the elastic modulus of the material can be calculated with the knowledge of the reduced modulus. Here, the values of E_i and ν_i were 1140 GPa and 0.07 for a diamond indenter tip [18].

2.5 Weight Loss

Weight loss of samples was assessed against the incubation time in PBS. Measurements were taken using an Ultra-Micro balance (Sartorius SE2). Measurements of all samples were taken before their incubation and after the samples had been dried in an oven (37°C; below the polymer glass transition temperature) for 48 hours to remove moisture. The weight loss was then calculated as a percentage using the following equation:

$$Weight\ loss\ (\%) = \frac{Change\ in\ weight}{Original\ weigh} \times 100\%. \quad (3)$$

2.6 Gel Permeation Chromatography (GPC)

GPC, also referred to size exclusion chromatography (SEC), allows for size-based separation of molecules in solution. GPC was used to assess the changes in molecular weight of the structure with degradation time. The ring section of Absorb stent was dissolved in the eluent at a concentration of 1 mg/ml. A 100 μl injection volume was used for each sample. It was ensured that the ring sections were fully dissolved prior to injection onto the column. GPC measurements were obtained in $CHCl_3$ + 2% triethylamine (TEA) at a flow rate of 1 mL/min, on a set of two PLgel 5 μm Mixed C columns plus a guard column, using a refractive index detector. Both the RI detector and columns were held at 40°C. Cirrus SEC software was used to analyse the data using polystyrene (PS-M) standards.

2.7 Differential Scanning Calorimetry (DSC)

DSC is acknowledged as the preferred technique to understand the thermodynamic changes in a polymer. This process assesses the apparent molar heat capacity of a macromolecule as a function of temperature. Through manipulation of temperature, a whole visualization of the thermodynamic character of the material can be obtained [19]. Here, rings were sectioned from the whole stent, with a mass of 2.9240 mg, for testing in a DSC system (Universal V4, TA instruments).

3. Results

3.1 Surface Profilometry

Surface profilometry was used to assess the surface properties of polymeric stent after manufacturing as well as at different stages of the *in vitro* degradation process. Fig. 3a illustrates the stent surface captured, where the black regions are redundant space. The redundant region, along with surface curvature, was subsequently removed to produce an area which can then be analysed

in two directions of interest, i.e., west to east (i.e., direction 1) and north to south (i.e., direction 2) as shown in Fig. 3b. The assessed area was then converted into a series of profiles so that an average surface roughness of the sample was obtained in comparison to a solo profile reading. Fig. 3c shows the series of profiles for the assessed area, with the average profile highlighted in blue. Three random areas of the stent surface were investigated with a size of 200×200 μm^2, from which averages were taken (Table 1).

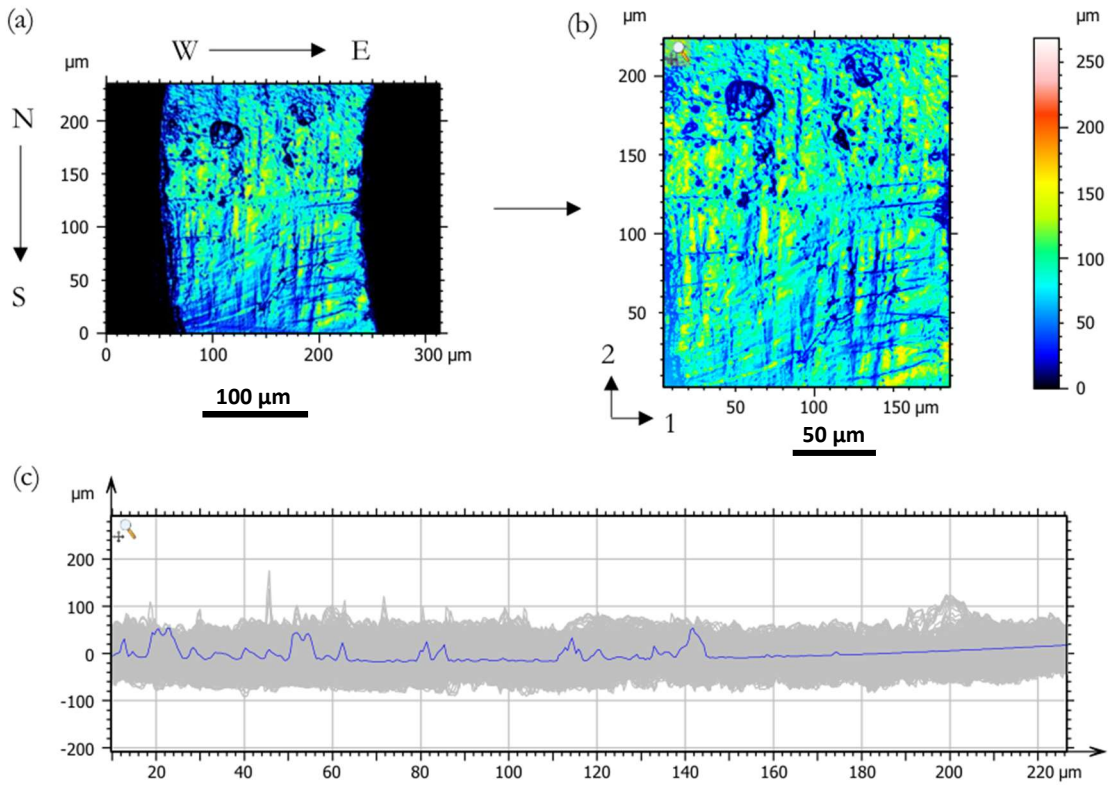

Figure 3, (a) Stent area scanned with optical profilometer, (b) surface area after removal of outlying area, and (c) typical series of profiles for the assessed area.

Table 1, Roughness data for stent surface (E → W = East to west; N → S = North to south)

Month	Direction	Average Ra	S.D.
0	W → E	0.155	0.0376
0	N → S	0.154	0.0508
12	W → E	21.1	4.68

12	N → S	21	4.75
18	W → E	18.4	5.21
18	N → S	12.3	2.65
24	W → E	8.26	3.53
24	N → S	9.45	1.26

From Table 1, it can be ascertained that the roughness of the stent in both directions remains consistent. The stent initially had a very low surface roughness, as a result of manufacturing process. With increasing degradation time, there is an observed increase in surface roughness at month 12 and then declining between month 12 and 24 as shown in Fig. 4. Although the roughness peaks at 12 months, it is not expected to affect the device performance as, by this time point, the stent is fully integrated into the vessel wall. When assessing the optical images of the stent between month 0 and 24 (Fig. 5), there seems no obvious visual evidence of surface erosion.

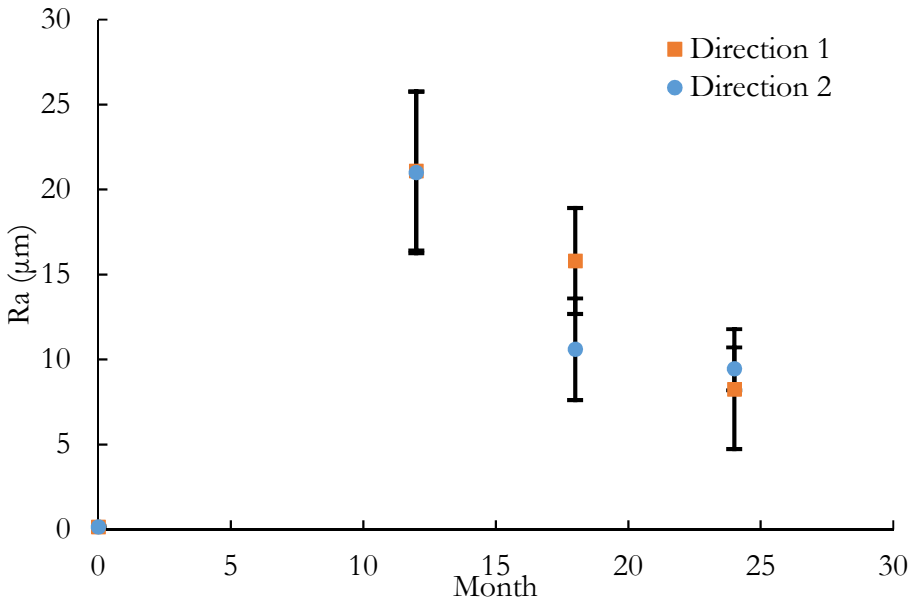

Figure 4, Evolution of surface roughness for the stent with degradation.

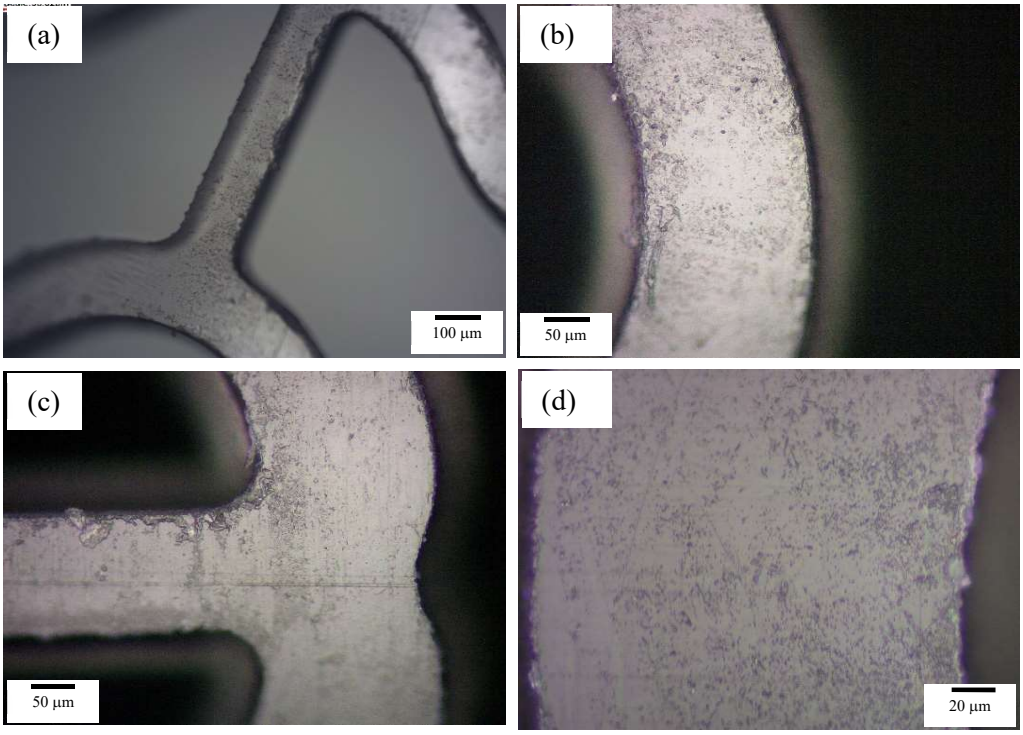

Figure 5, Optical images of stent surface of (a) virgin, (b) 12-month, (c) 18-month and (d) 24-month samples.

3.2 Weight Loss and Chemical Analyses

3.2.1 Weight loss

The weight loss is indicative of the loss of smaller polymer sections formed due to chain scission, leaving behind the core of the material. This is a feature of bulk degradation, which the aliphatic polyesters, such as PLLA, normally undergo [20]. Fig. 6 shows the percentage of weight loss for the samples (Equation (3)). Before measurements, drying process was carried out at a temperature (37°C) below the glass transition temperature Tg, therefore not affecting the material by additional thermal degradation. Only one sample was measured for each month due to the limited amount of tubing and stents available for this study. The results obtained in this study concur with bulk degradation in polymers, due to the extremely limited amount of weight loss. This could even be construed as negligible, as weight loss remained below 2% of the sample's initial weight. These results agree with multiple studies [21-24], where no significant weight changes were found for

solid PLLA with *in vitro* degradation during a substantial portion of the time scale expected for full resorption of the device within the body.

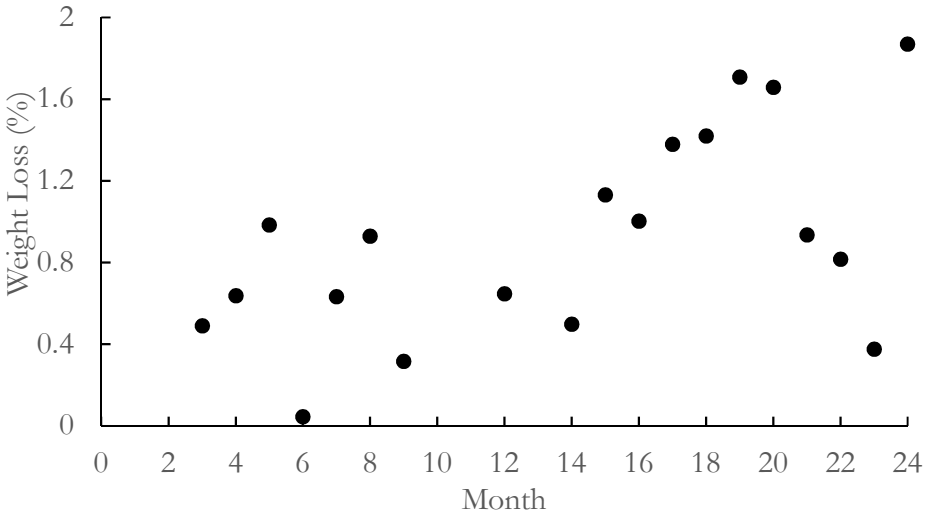

Figure 6, Weight loss with degradation over a 2-year period.

3.2.2 Molecular weight change

Fig. 7 illustrates the GPC curves at 0, 12, 15 and 18 months. Data presented here correspond to elution of the polymer between approximately 10 and 16 minutes. A change in the chemical composition is manifested as a shift to a later elution time and a larger peak for the degraded samples. Later elution corresponds to the presence of molecules with a reduced chain length and molecular weight, which is anticipated due to chain scission during degradation. This is corroborated with the data presented in Table 2, where the molecular weight of the highest peak drops drastically from 0 to 21 months (by 65%) and the molecular weight (*Mn* and *Mw*) also depletes. The polydispersity index, which is used as a measure of the breadth of the molecular weight distribution and defined as *Mw*/*Mn* [25], remained almost constant over the course of two years of *in vitro* degradation. Concentration of the samples was consistent across all testing. It can be said with certainty here that there was degradation taking place due to the decline in molecular weight of the material [24].

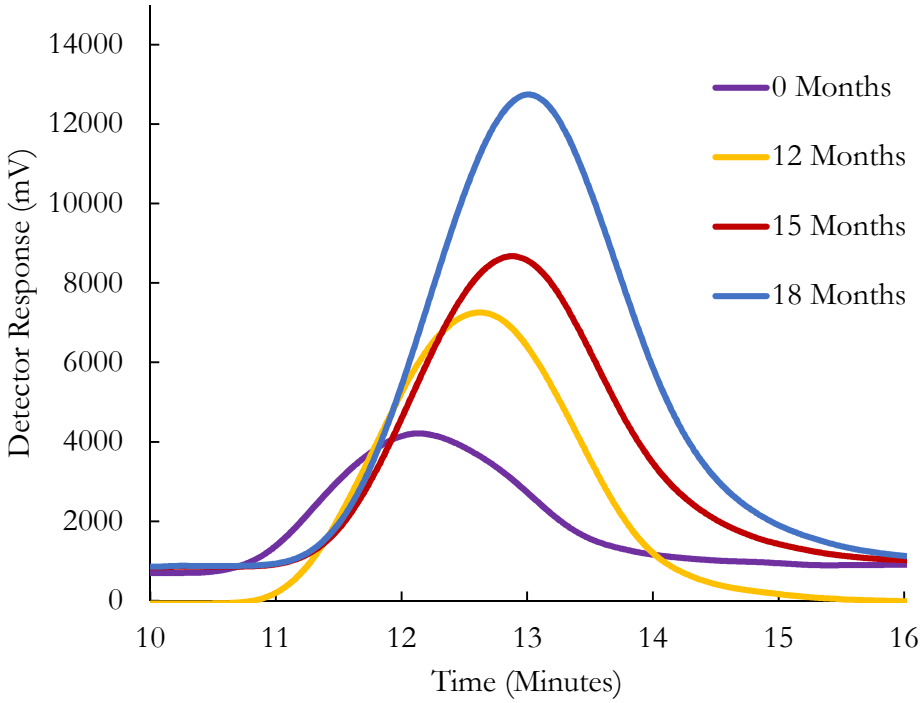

Figure 7, Effect of degradation on raw molecular weight detected by GPC.

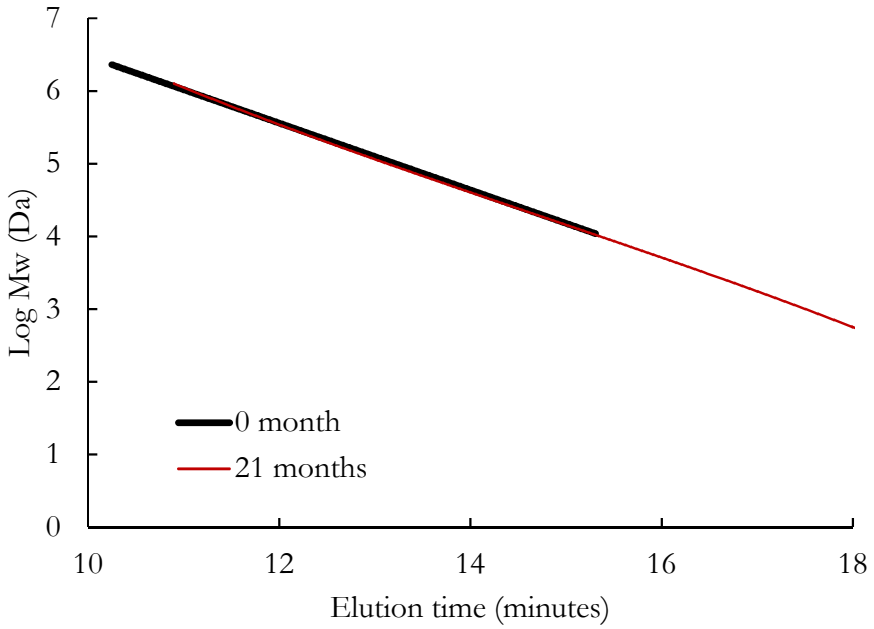

Figure 8, Standard plot of log Mw with elution time.

Table 2, Data obtained from the GPC analyses with molecular weight normalised to that at virgin state (month 0).

Month	0	12	15	18	21
Normalised molecular weight at the peak (Mp)	1.0	0.55	0.38	0.36	0.35
Normalised number average molecular weight (Mn)	1.0	0.66	0.49	0.42	0.41
Normalised weight average molecular weight (Mw)	1.0	0.65	0.48	0.43	0.41
Polydispersity index (PD)	2.00	1.97	1.97	2.04	2.01

The logarithm of molecular weight against the elution time is plotted in Fig. 8, where a typical linear trend is seen at both time points. These results agree with those in Fig. 7, where products of degradation are present due to the shift in elution time, corresponding to lower molecular weight chains. There are 3 stages of degradation for aliphatic polyester polymers which undergo bulk hydrolytic degradation: (1) second order hydrolysis, (2) auto-acceleration and (3) dissolution of degradation products [22]. For the period over which the stent was exposed to *in vitro* conditions, it seems that the specimen was in either of the first 2 stages of degradation as there was no obvious weight loss. This correlates well with the results for molecular weight. Basically, although there was no obvious weight loss, there was an obvious decline in molecular weight of the PLLA chains. This confirms that degradation and chain scission are occurring; however, the smaller chains are not able to diffuse out of the sample, therefore explaining the negligible weight loss.

3.2.3 Crystallinity variation

As established in previous work, DSC is a preferred technique to assess thermodynamic changes in a polymer. Here the procedure was conducted to assess the thermal properties of the degraded samples and ultimately their crystallinity percentage over *in vitro* degradation. As seen in Table 3, from the beginning to the end of the degradation period (2 years), the sample crystallinity increased

by 25.9%, which corresponds to the bulk degradation mechanism for aliphatic polyesters such as PLLA. Basically, the amorphous regions are the first to succumb to attack by hydrolytic degradation, thereby increasing the sample crystallinity with degradation time [23, 24]. Based on the continual increase in sample crystallinity over the 2-year period, it can be said that degradation was in the mid-phase for these *in vitro* samples, as its decline in crystallinity would be expected after the peak when the shorter polymer chains start to move out of the sample. Overall, the results from DSC, GPC and weight loss analyses agree with one another. It should be noted that the samples were not dried in vacuum, which could give an overestimation of crystallinity due to the occurrence of oxidation in the drying process.

Table 3, DSC data for degraded samples

Sample (months)	Enthalpy of melt (J/g)	Crystallinity (%)
0	52.68	56.66
12	70.7	76.02
18	77.01	82.87
24	79.57	82.56

3.3 Mechanical Characterisation

3.3.1 AFM measurements

AFM allows for interrogation of a sample surface at shallow indentation depths. Tang *et al.* [16] proposed a method to quantitatively measure the elastic modulus of a material using AFM, where the unloading portion of the load-displacement curve was used to assess the modulus (Section 2.3). Figs. 9a-c shows the unloading curves obtained with AFM for samples which underwent degradation for 18 months. Results are presented at a 6-month interval. The results here suggested

that there was no significant difference in material response between the three locations of interest, confirming the consistency of the surface layers of the sample (up to 200 nm according to AFM).

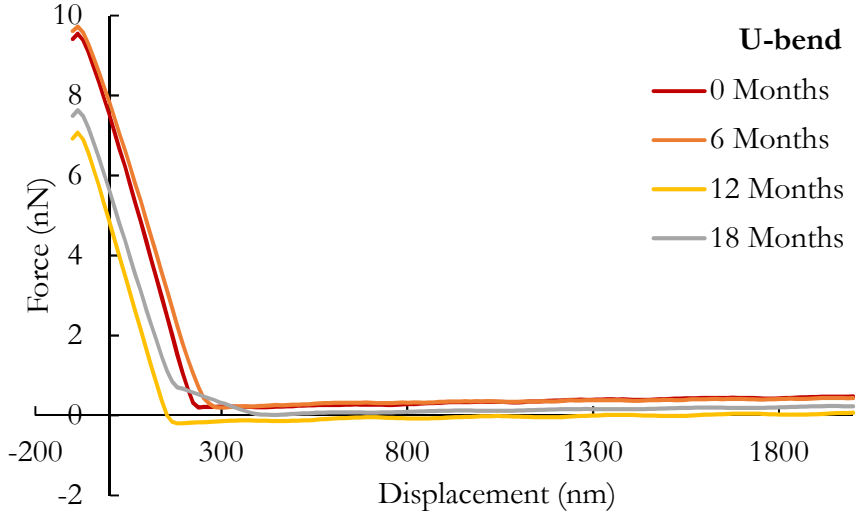

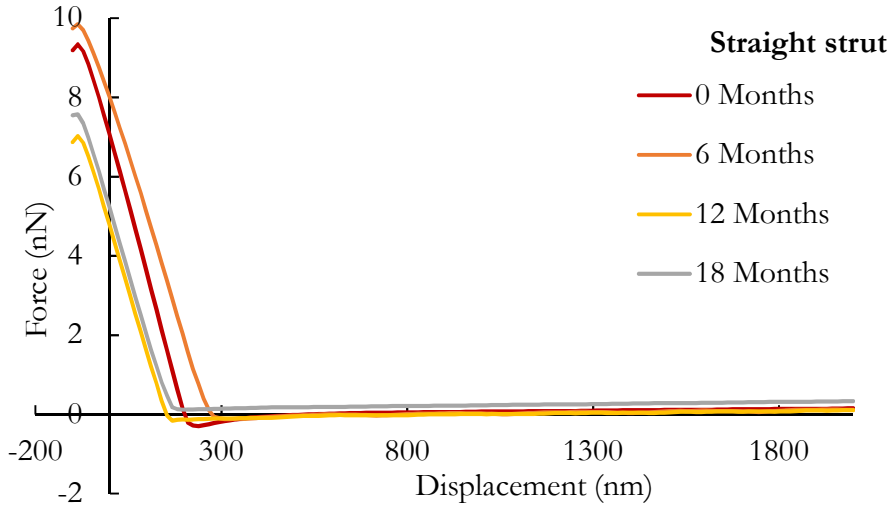

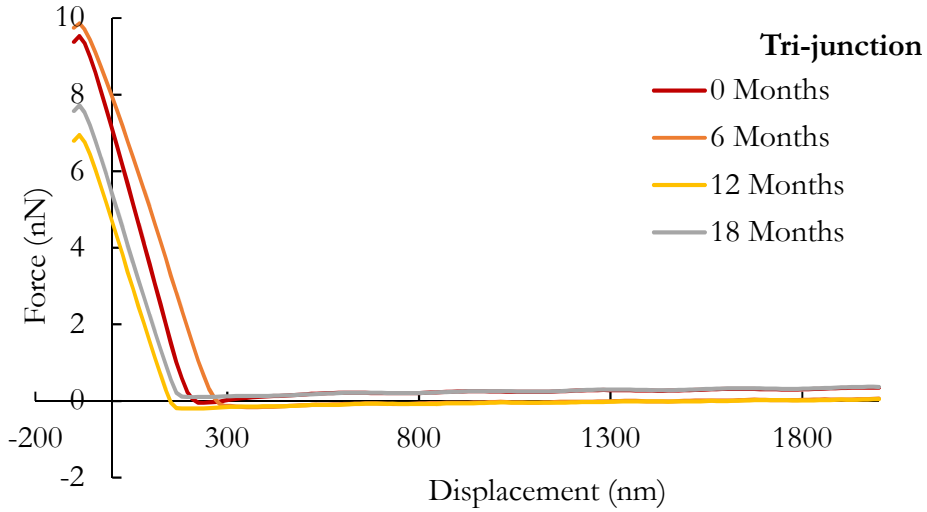

Figure 9, AFM results at 3 different locations with degradation

Fig. 10 shows the average elastic modulus, with error bars, for each sample, and provides a representation of the surface layer behaviour, due to the shallow 200 nm indentation depth, over *in vitro* degradation times. There appears to be no dramatic changes to the modulus over time, which is as expected due to the prolonged degradation life that PLLA presents *in vitro*. These results back up those of weight loss, as there is no reduction in the weight and the samples still possessed material integrity. Additionally, this is concurrent with the degradation mechanism of PLLA, i.e., bulk degradation taking place while the surface layers of the material remain intact.

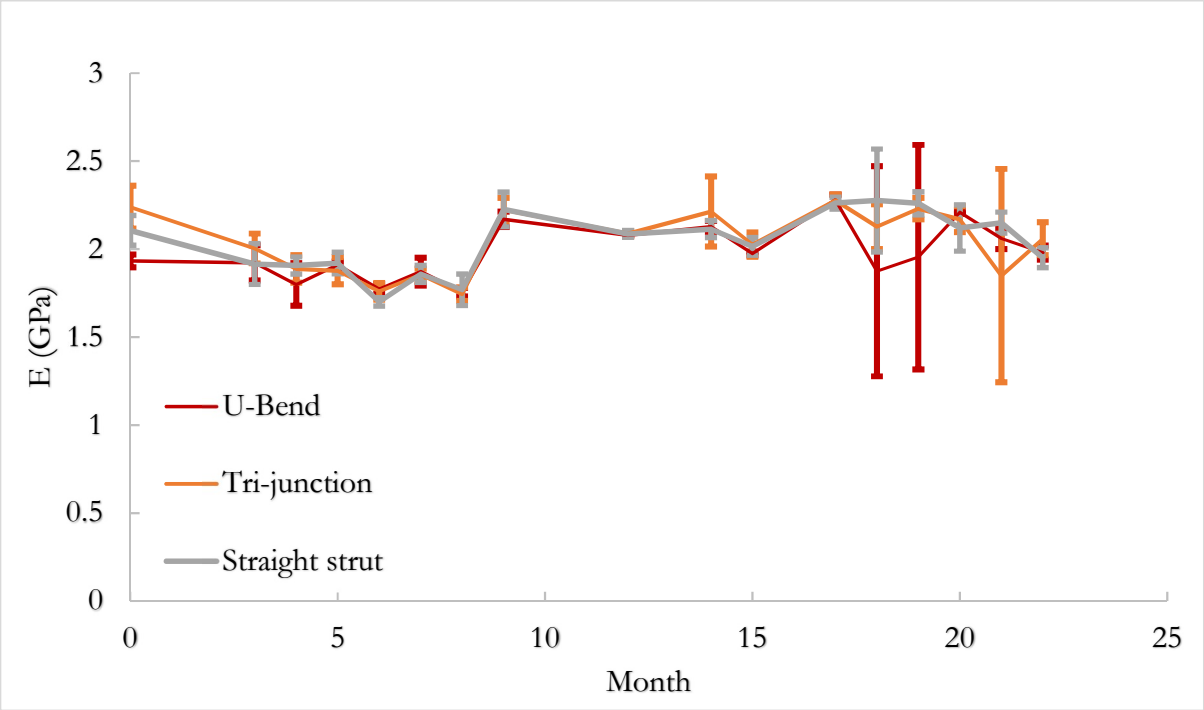

Figure 10, Evolution of surface elastic modulus over two-year *in vitro* degradation

The values presented in Table 4 are an average of 20 indents, which were taken at random locations over each area. The modulus over the two-year period changed in a range between 1.70 and 2.28 GPa, with a fluctuation of 0.5 GPa. On closer inspection of Fig. 10, the modulus values were not constant. The irregular pattern could be assigned to numerous factors. AFM measures properties

on a nanoscale, while polymer chains are generally on an angstrom scale. As a result of this size mismatch, the variation in both standard deviation and modulus over time was due to spatial non-uniformity of the molecular structure. As illustrated in Fig. 11, it is possible for indents to be made in a single-phase area of the polymer, i.e., amorphous, crystalline or spherulite region. The work by Iqbal *et al.* [26] showed that it is possible that indentation at a crystalline polymer chain could yield mechanical properties significantly different from indentation at amorphous area, which is referred as the bi-modal response of polymers.

Table 4, Average Young's modulus values (GPa) of 20 indents for each location.

Month	U-bend	Tri-junction	Straight strut
0	1.93	2.24	2.11
3	1.92	2.00	1.92
4	1.80	1.89	1.91
5	1.91	1.88	1.92
6	1.77	1.76	1.70
7	1.87	1.86	1.86
8	1.76	1.74	1.77
9	2.17	2.22	2.23
12	2.08	2.09	2.09
14	2.13	2.21	2.11
15	1.97	2.03	2.01
17	2.28	2.28	2.26
18	1.87	2.13	2.28
19	1.95	2.23	2.26
20	2.21	2.17	2.12
21	2.06	1.85	2.15
22	1.98	2.06	1.95
23	2.04	2.04	1.97
24	1.85	1.92	1.93

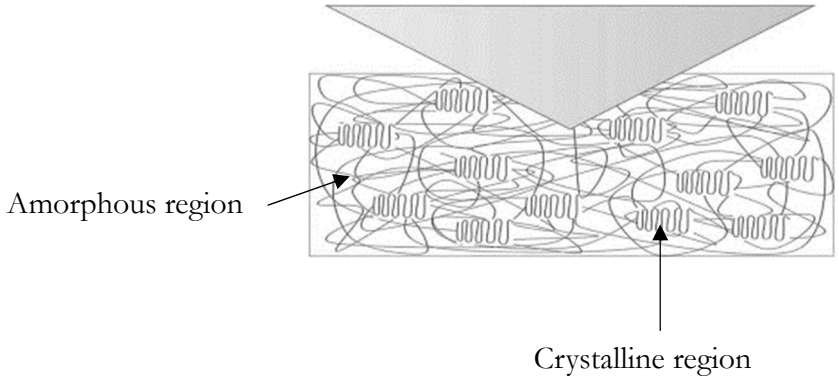

Figure 11, Schematic of AFM indentation into a semi-crystalline material, where it is possible to indent different regions.

3.3.2 Nanoindentation measurements

Nanoindentation allows for assessment of material properties at depths greater than AFM, aiming to ascertain changes in mechanical properties of the material over degradation at a larger scale. Initially, a range of depths were investigated by varying the load used for indentation with a Berkovich indenter in order to select the ideal parameters for main experiments. Fig. 12 illustrates the force-displacement curves, with differing indentation loads, for an 18-month sample. There are no similar trends for loading or unloading curves with each indent. This is particularly significant for the unloading curve as its top portion is used to calculate the Young's modulus of the material using the Oliver-Pharr theory. Table 5 compares the data for 4 indents which were carried out on the same 18-month sample using the same testing set up. Here we can see the wide variation of mechanical properties, with a difference of 1.45 GPa between the largest and the smallest Young's modulus values obtained from indentation in a small region. What should be noted here additionally is that these results were produced at the same load, but with drastically different maximum indentation depths. As discussed for AFM (Fig. 11), indentation is generally specific to areas within the polymer. For nanoindentation, a sharp tip such as the three-sided Berkovich tip can cause an internal shift of polymer chains, leading to such obscure results.

Increase in chain mobility as a result of the shortening of polymer chains, due to their scission with degradation, would be a reason for result inconsistency. The shorter chains could also cause the increase in material elasticity seen with degradation. Another factor could be a gradient of mechanical properties through the cross section of the stent, linked with bulk degradation and/or manufacturing process.

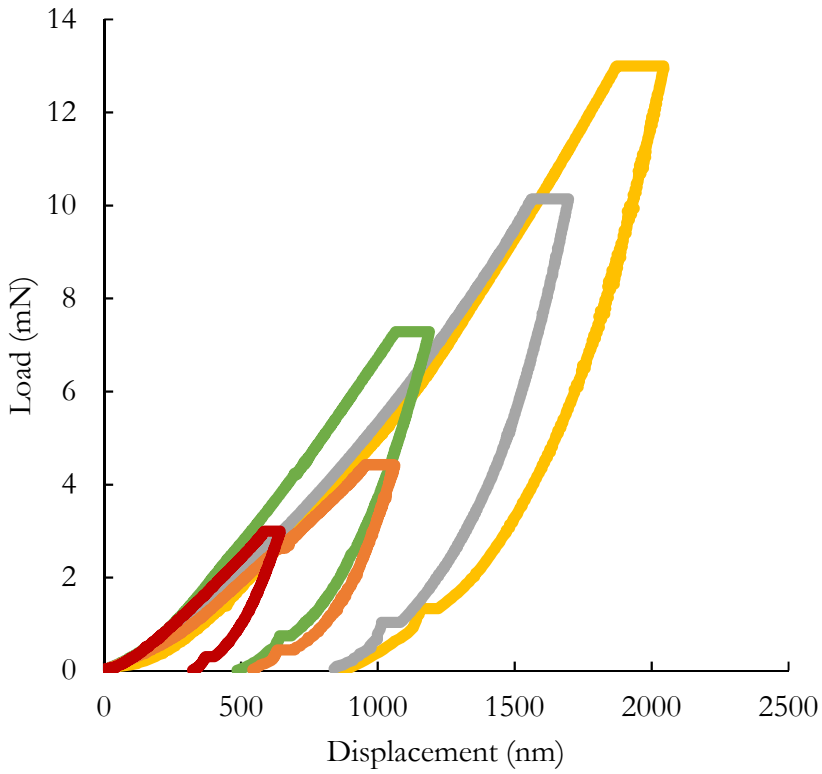

Figure 12, Illustration of variation in curves with varying loads for an 18-month sample

Table 5, Data comparison for indentation made on the sample at four different locations under the same load (23 mN).

Max. depth (nm)	Residual depth (nm)	Plastic deformation (%)	Hardness (GPa)	Reduced modulus Er(GPa)	Young's modulus E (GPa)	Contact compliance (nm/mN)
3482.9	3109.4	89.28	0.097	2.66	2.32	21.65
2246.2	1922.2	85.57	0.254	4.96	4.33	18.78
3868.1	2694.5	69.66	0.129	0.98	0.85	68.04

3921.8	2825.1	72.03	0.118	1.00	0.87	63.58

Fig. 13 shows the span of the modulus which were obtained from indentation between 10 mN and 23 mN on the stent ring samples. There is a large variation in the results due to the two-phase structure of PLLA, as illustrated in Fig. 11. As discussed in Section 3.3.1 for AFM, it is possible for indents to be made in a single-phase area of the polymer, i.e., amorphous, crystalline or spherulite region. Indentation at a crystalline polymer chain could yield mechanical properties significantly different from indentation at amorphous area [26]. Overall, a decline can be seen in the modulus from month 0 to month 15, followed by an increase at month 18 and a continued decline afterwards. As discussed above (Table 3), differential scanning calorimetry yielded a crystallinity of 82.27% at Month 18, and there is an 82.27% chance of indenting in crystalline region, resulting in higher Young's modulus. Factors such as sample preparation and the variation of rings used for indentation may further increased this chance. Overall, the results could be seen as a trend of degradation; however, at this point, further investigation is currently ongoing to draw a definitive conclusion, especially by exploring an alternative spherical nanoindentation technique which may overcome the issues related with the bimodal structure of PLLA. Furthermore, the moduli for all the samples, obtained at various degradation times, are presented in Fig. 14 against the plastic deformation which was calculated as (residual depth/maximum depth)×100%. A pattern is observed for all the samples, where the obtained moduli sit in one of the two regions, corresponding to either amorphous or crystalline structure of the material.

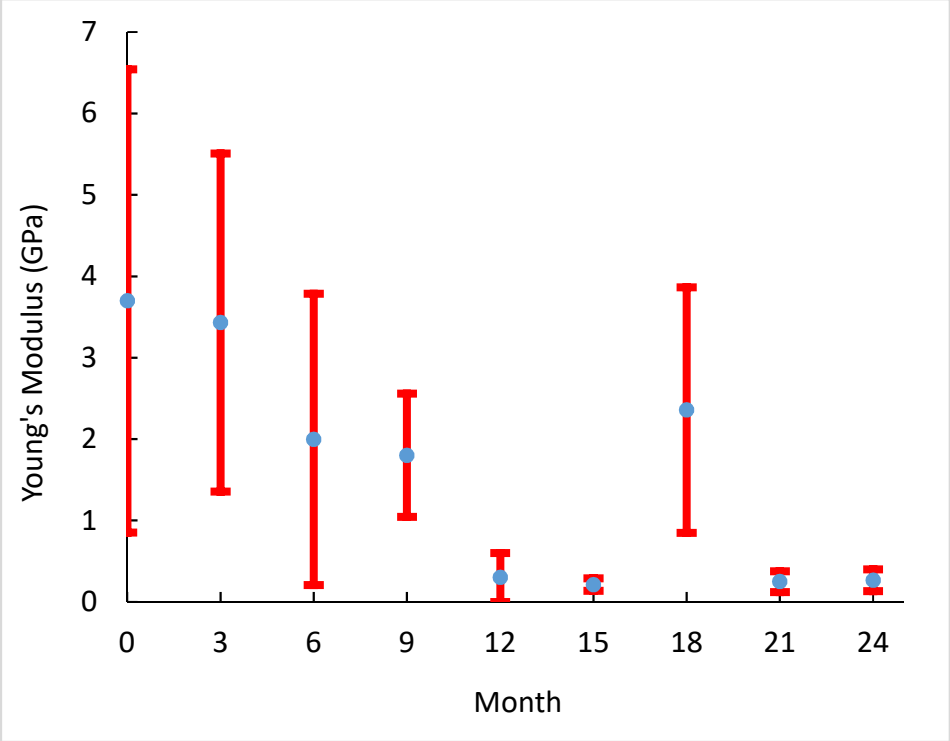

Figure 13, Data obtained for indentation on each sample during degradation.

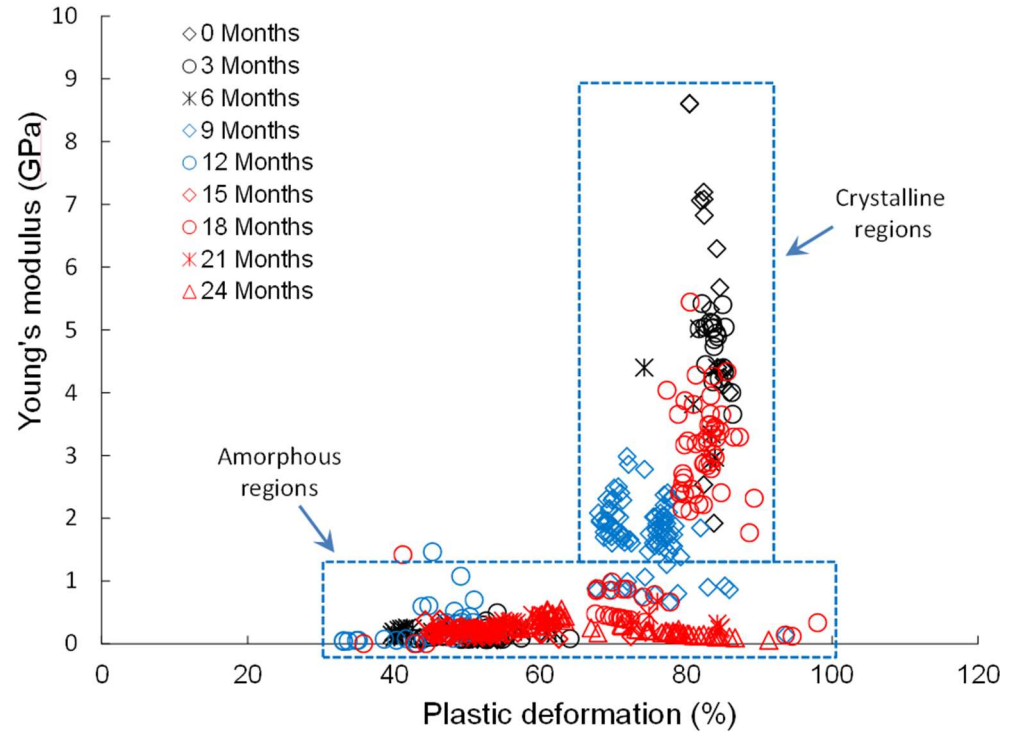

Figure 14, Young's modulus *vs.* material plasticity at different degradation times.

4. Discussions

To the best of our knowledge, nanoindentation was not used previously to assess the mechanical properties of polymeric stent rings. It can be deduced that pyramidal indentation of polymeric materials makes it a challenge to interpret the change of the material properties over *in vitro* degradation. Even at consistent loads, different penetration depths into the material were reached, therefore yielding different mechanical properties. As shown in Table 5, the penetration depth varied between 2.2 μm and 3.9 μm under under a 23 mN load, resulting in different modulus values. Shallower indents align with higher elastic modulus and deeper indents deliver lower modulus, which could be a signature of indentation size effect (ISE), intrinsic behaviour of materials under nanoindentation. When assessing nanoindentation as a method for capturing the degradation of PLLA stents, it can be concluded that this is a localized method of analysis and largely affected by the semi-crystalline structure of the material. The variability of degradation results obtained from pyramidal indentation can also be attributed to the material's non-homogenous properties across the whole stent, related to the manufacturing process. Taking all these considerations into account, quantification of degradation effects on stent mechanical properties cannot be made solely with pyramidal nanoindentation. So, effects of material degradation, non-uniformity of the polymer chain alignment and testing methodology (i.e., ISE) cannot be separated in this case, and consequently, additional techniques such as spherical nanoindentation and/or structural testing [27] need to be sought in order to deliver more consistent measurements of the material properties over degradation.

In this study, multiple indents were randomly taken across the sample surface to obtain a large data set. For the values of modulus, standard deviations were calculated to quantify the amount of dispersion of the data obtained, for both AFM and nanoindentaion. This has been provided in Tables 6 to 9. Each table lists the mean and maximum/minimum values of the measurements at different degradation times, with the values of standard deviation (SD). It can be seen that AFM

measurements (Tables 6 to 8) gave less variations than nanoindentation measurements (Table 9), as also reflected in Figs. 10 and 13. As discussed above, this is associated with the difference in penetration depths for the two methods as well as the bulk degradation nature of PLLA.

Table 6, Statistical data for modulus obtained with AFM for straight strut.

Straight	0	3	6	9	12	15	18	20	22	24
Min	2.00	1.80	1.67	2.06	2.06	1.93	2.05	1.97	1.84	1.88
Max	2.21	2.34	1.73	2.27	2.11	2.06	2.85	2.30	2.00	1.94
Mean	2.106	1.915	1.700	2.225	2.086	2.015	2.276	2.12	1.951	1.920
SD	0.084	0.116	0.024	0.098	0.019	0.050	0.292	0.131	0.056	0.022

Table 7, Statistical data for modulus obtained with AFM for U-bend strut.

U-bend	0	3	6	9	12	15	18	20	22	24
Min	1.81	1.76	1.72	2.09	2.03	1.95	1.79	2.19	1.98	1.55
Max	1.96	2.01	1.79	2.2	2.12	1.98	2.22	2.22	2.02	1.93
Mean	1.932	1.922	1.773	2.168	2.078	1.974	1.873	2.21	1.98	1.846
SD	0.036	0.099	0.028	0.044	0.001	0.011	0.596	0.001	0.039	0.140

Table 8, Statistical data for modulus obtained with AFM for tri-junction strut.

Junction	0	3	6	9	12	15	18	20	22	24
Min	2.07	1.86	1.68	2.12	2.05	1.94	2.23	2.03	1.93	1.88
Max	2.40	2.06	1.82	2.29	2.1	2.12	2.87	2.25	2.18	1.95
Mean	2.238	2.003	1.759	2.224	2.087	2.025	2.127	2.17	2.058	1.920
SD	0.121	0.084	0.047	0.066	0.015	0.069	0.127	0.073	0.093	0.022

Table 9, Statistical data for modulus obtained with nanoindentation (stent ring).

Month	0	3	6	9	12	15	18	21	24
Min	0.007	0.086	0.116	0.521	0.047	0.039	0.0004	0.111	0.057
Max	8.601	5.401	7.000	2.031	1.465	0.244	5.442	0.667	0.537
Mean	3.698	3.431	1.995	1.801	0.300	0.213	2.356	0.249	0.265
SD	2.844	2.076	1.790	0.757	0.301	0.077	1.507	0.126	0.134

Biosafety, both chemical and mechanical, is of primary importance for medical stents. Chemical safety is largely dependent on the choice of materials. The bioresorbable stent studied in this paper is made of PLLA which is biocompatible, non-toxic and unlikely to induce severe inflammation to the vessel [28]. Also, their degradation products are natural and can be cleared out of the human body safely. Mechanical damage is normally caused by the stenting process as high pressure is required to expand the stent inside the diseased artery via balloon inflation. This can impose severe deformation to vascular wall, resulting in mechanical damage of artery layers [29]. To improve biosafety, it is important to control bioresorption at a desirable and predictable rate, which can be achieved by tuning molecular weight, crystallinity and hydrophilicity of those polymers [30]. In addition, mechanical damage can be minimised by optimising the stent structure and altering the material properties, based on computational and experimental techniques [28, 29]. In this work, we are more focused on the chemical and mechanical degradation behaviours of a commercial PLLA stent over two-year *in vitro* conditions, and the results can be used to support the design and optimisation of future bioresorbable stents to improve the biosafety. It should be noted that a proper biosafety study will require different methodologies and techniques, which is beyond the scope of current study.

Recently, several independent clinical trials have raised the thrombosis issue associated with the long-term outcome (three years and beyond) of bioresorbable polymeric stents [31-34]. The exact cause of the problem has not been identified yet, but stent design and material are believed to play

important roles in the long-term performance of bioresorbable polymeric stents. As reported in Yamaji et al. [32], strut discontinuity caused by the loss of structural integrity during stent degradation was the leading mechanism of very late thrombosis for bioresorbable polymeric stents. In this case, one potential way to reduce the risk of thrombosis and debris shedding is to tailor the degradation rate, as well as control the change of mechanical properties, of bioresorbable polymeric stents through novel material processing and optimal structural design, with validation against thorough animal studies. Again, this will require a significant amount of additional effort and time, and is beyond the scope of current study.

5. Conclusions

In this paper, the mechanical properties of polymeric stent were assessed at nanoscale, on the surface as well as at a depth into the sample, which was not performed previously. The aim here was to assess the mechanical property change of the stent over degradation in manufactured states. No significant changes to the Young's modulus were observed with AFM due to bulk degradation nature of the polymer. It was also established that pyramidal indentation provided a range of modulus values for the material, with lower modulus values related to the amorphous areas of the stent while higher elastic modulus resulted from indentations made in the crystalline regions. There was a trend of reduction in modulus with *in vitro* degradation, but not continuous due to the limitation of pyramidal indentation in testing semi-crystalline polymers. GPC analyses showed an over 2-fold decrease in molecular weight after 21 months of *in vitro* degradation, despite of negligible weight loss. These results indicated the bulk-degradation mechanism in PLLA, without significant mass loss during the stages of degradation studied in this paper.

6. Competing interests

The authors declare that they have no competing interests

7. Acknowledgement

This work is funded by the British Heart Foundation PhD research project (Grant number: FS/15/21/31424; Title: Towards controlling the mechanical performance of polymeric bioresorbable vascular stent during biodegradation).

8. References

1. Ulery, B.D., Nair, L.S. & Laurencin, C.T. Biomedical applications of biodegradable polymers. *J. Polym. Sci. B. Polym. Phys.* **49,** 832–864 (2011).
2. Blair, R.W., Dunne, N.J., Lennon, A.B. & Menary, G.H. Processing-property relationships of biaxially stretched poly(L-lactic acid) sheet for application in coronary stents. *J. Mech. Behav. Biomed. Mater.* **86**, 113–121 (2018).
3. Wang, Q., Fang, G., Zhao, Y., Wang, G. & Cai, T. Computational and experimental investigation into mechanical performances of Poly-L-Lactide Acid (PLLA) coronary stents, *J. Mech. Behav. Biomed. Mater.* **65**, 415–427 (2017).
4. Quynh, T.M., Mitomo, H., Nagasawa, N., Wada, Y., YoshiiQ, F. & Tamada, M. Properties of crosslinked polylactides (PLLA & PDLA) by radiation and its biodegradability. *Eur. Polym. J.* **43,** 1779-1785 (2007).
5. Wang, Y. & Zhang, X. Vascular restoration therapy and bioresorbable vascular scaffold. *Regen. Biomater.* **1,** 49–55 (2014).
6. Göpferich, A. Mechanisms of polymer degradation and erosion. *Polym. Scaffolding Hard Tissue Eng.* **17,** 103–114 (1996).
7. Vieira, A.C., Vieira, J.C., Ferra, J.M., Magalhães, F.D., Guedes, R.M., Marques, A.T. Mechanical study of PLA–PCL fibers during *in vitro* degradation. *J. Mech. Behav. Biomed. Mater.* **4**, 451-460 (2011).
8. Gong, Y., Zhou, Q., Gao, C. & Shen, J. *In vitro* and *in vivo* degradability and cytocompatibility of poly(l-lactic acid) scaffold fabricated by a gelatin particle leaching method. *Acta Biomater.* **3,**

531–540 (2007).

9. Yuan, X., Mak, A.F.T. & Yao, K. *In vitro* degradation of poly(L- lactic acid) fibers in phosphate buffered saline. *J. Appl. Polym. Sci.* **85,** 936–943 (2002).
10. Nuutinen, J.P., Valimaa, T., Clerc, C. & Tormala, P. Mechanical properties and *in vitro* degradation of bioresorbable knitted stents. *J. Biomater. Sci. Polym. Ed.* **13**, 1313-1323 (2002).
11. Zilberman, M., Nelson, K.D. & Eberhart, R.C. Mechanical properties and *in vitro* degradation of bioresorbable fibers and expandable fiber-based stents. *J. Biomed. Mater. Res. Part B Appl. Biomater.* **74B,** 792–799 (2005).
12. Bartkowiak-Jowsa, M., Będziński, R., Kozłowska, A., Filipiak, J. & Pezowicz, C. Mechanical, rheological, fatigue, and degradation behavior of PLLA, PGLA and PDGLA as materials for vascular implants. *Meccanica* **48,** 721–731 (2012).
13. Luo, Q., Liu, X., Li, Z., Huang, C., Zhang, W., Meng, J., Chang, Z. & Hua, Z. Degradation model of bioabsorbable cardiovascular stents. *PLoS One* **9,** e110278 (2014).
14. Cifuentes, S.C., Frutos, E., Benavente, R., González-Carrasco, J.L. & Lorenzo, V. Strain rate effect on semi-crystalline PLLA mechanical properties measured by instrumented indentation tests. *Eur. Polym. J.* **59,** 239–246 (2014).
15. Ghosh, S., Viana, J.C., Reis, R.L. & Mano, J.F. Effect of processing conditions on morphology and mechanical properties of injection-molded poly(l-lactic acid). *Polym. Eng. Sci.* **47,** 1141–1147 (2007).
16. Tang, B., Ngan, A.H. & Pethica, J.B. A method to quantitatively measure the elastic modulus of materials in nanometer scale using atomic force microscopy. *Nanotechnol.* **19,** 495713 (2008).
17. Oliver, W. C. & Pharr, G. M. An improved technique for determining hardness and elastic modulus using load and displacement sensing indentation experiments. *J. Mater. Res.* **7,** 1564–1583 (1992).
18. Ozcivici, E., Ferreri, S., Qin, YX. & Judex, S. Determination of bone's mechanical matrix properties by nanoindentation. In: Westendorf J.J. (eds) Osteoporosis. Methods In Molecular

Biology™, vol 455. Humana Press (2008)

19. Freire, E. Differential scanning calorimetry. In: Shirley B.A. (eds) Protein stability and folding. Methods in Molecular Biology™, vol 40. Humana Press (1995).

20. Tesfamariam, B. Bioresorbable vascular scaffolds: Biodegradation, drug delivery and vascular remodelling. *Pharmacological Research* **107**, 163-171 (2016).

21. Gaona L.A., Gómez Ribelles, J.L., Perilla, J.E. & Lebourg, M. Hydrolytic degradation of PLLA/PCL microporous membranes prepared by freeze extraction. *Polym. Degrad. Stab.* **97,** 1621–1632 (2012).

22. Lyu, S. & Untereker, D. Degradability of polymers for implantable biomedical devices. *Int. J. Mol. Sci.* **10,** 4033–4065 (2009).

23. Dreher, M.L., Nagaraja, S. & Batchelor, B. Effects of fatigue on the chemical and mechanical degradation of model stent sub-units. *J. Mech. Behav. Biomed. Mater.* **59**, 139-145 (2016).

24. Liao, L., Peng, C., Li, S., Lu, Z. & Fan, Z. Evaluation of bioresorbable polymers as potential stent material - In vivo degradation behavior and histocompatibility. *J. Appl. Polym. Sci.* **134***,* 44355 (2017).

25. Rane, S.S. Polydispersity index: how accurately does it measure the breadth of the molecular weight distribution? Chem. Mater. **17**, 926–926 (2005).

26. Iqbal, T., Briscoe, B.J., Yasin, S. & Luckham, P.F. Nanoindentation response of poly(ether ether ketone) surfaces-A semicrystalline bimodal behavior. *J. Appl. Polym. Sci.* **130,** 4401-4409 (2013).

27. Kimble, L.D. & Bhattacharyya, D. In vitro degradation effects on strength, stiffness, and creep of PLLA=PBS: A potential stent material. *Int. J. Polym. Mater. Polym. Biomater.* **64**, 299-310 (2015).

28. Hu, T., Yang, C., Lin, S., Yu, Q. & Wang, G. Biodegradable stents for coronary artery disease treatment: Recent advances and future perspectives. *Mater. Sci. Eng. C* **91**, 163-178 (2018).

29. Schiavone, A., Abunassar, C., S. Hossainy, S. & Zhao, L.G. (2016) Computational analysis of

mechanical stress-strain interaction of a bioresorbable scaffold with blood vessel. *J. Biomech.* **49**, 2677-2683 (2016).

30. Onuma, Y., Ormiston, J. & Serruys, P.W. Bioresorbable scaffold technologies. *Circ. J.* **75**, 509-520 (2011).

31. Kimura, T., Kozuma, K., Tanabe, K., Nakamura, S., Yamane, M., Muramatsu, T., Saito, S., Yajima, J., Hagiwara, N., Mitsudo, K., Popma, J.J., Serruys, P.W., Ying, S.H., Cao, S., Staehr, P., Cheong, W.F., Kusano, H. & Stone, G.W. A randomized trial evaluating everolimus-eluting absorb bioresorbable scaffolds vs. everolimus-eluting metallic stents in patients with coronary artery disease: Absorb Japan. *Eur. Heart J.* **36**, 3332-3342 (2015).

32. Yamaji, K., Ueki, Y., Souteyrand, G., Daemen, J., Wiebe, J., Nef, H., Adriaenssens, T., Loh, J.P., Lattuca, B., Wykrzykowska, J.J., Gomez-Lara, J., Timmers, L., Motreff, P., Hoppmann, P., Abdel-Wahab, M., Byrne, R.A., Meincke, F., Boeder, N., Honton, B., O'Sullivan, C.J., Ielasi, A., Delarche, N., Christ, G., Lee, J.K.T., Lee, M., Amabile, N., Karagiannis, A., Windecker, S. & Räber, L. Mechanisms of very late bioresorbable scaffold thrombosis: the INVEST registry. *J. Am. Coll. Cardiol.* **70**, 2330-2344 (2017).

33. Xu, B., Yang, Y., Han, Y., Huo, Y., Wang, L., Qi, X., Li, J., Chen, Y., Kuo, H., Ying, S., Cheong, W., Zhang, Y., Su, X., Popma, J., Gao, R. & Stone, G.W. Comparison of everolimus-eluting bioresorbable vascular scaffolds and metallic stents: three-year clinical outcomes from the ABSORB China randomised trial. *Eurointervention* **14**, 554-561 (2018).

34. Torrado, J., Buckley, L., Durán, A., Trujillo, P., Toldo, S., Raleigh, J.V., Abbate, A., Biondi-Zoccai, G. & Guzmán, L.A. Restenosis, stent thrombosis, and bleeding complications: navigating between Scylla and Charybdis. *J. Am. Coll. Cardiol.* **71**, 1676-1695 (2018).